ELECTROMECHANICAL DYNAMICS SIMULATIONS OF SUPERCONDUCTING LSM ROCKET LAUNCHER SYSTEM IN ATTRACTIVE - MODE

Kinjiro Yoshida, Kengo Hayashi, Hiroshi Takami
Depart. of Electrical Engineering
Faculty of Engineering, Kyushu University
10 - 1 6-chome Hakozaki Higashi - ku
Fukuoka, 812 JAPAN

SUMMARY

Further feasibility study on a superconducting linear synchronous motor (LSM) rocket launcher system is presented on the basis of dynamic simulations of electric power, efficiency and power factor as well as the ascending motions of the launcher and rocket. The advantages of attractive-mode operation are found from comparison with repulsive-mode operation. It is made clear that the LSM rocket launcher system, of which the long-stator is divided optimally into 60 sections according to launcher speeds, can obtain high efficiency and power factor.

INTRODUCTION

In previous papers [1], [2], we proposed a vertical type superconducting linear synchronous motor (LSM) rocket launcher system of which four acceleration guideways with double-layer armature-windings are arranged symmetrically along a shaft of about 1,500 m under the ground. From our feasibility study, it was found that the linear launcher made the rocket attain the speed of 700 km/h at the height of 100 m above the ground, at which the payload could be increased more than 15 % by substituting it for the first-step acceleration rocket. The novel armature-current control method proposed previously by us was successfully applied in a repulsive-mode operation to ascend and guide simultaneously the linear launcher with control of the Coriolis force. The current control method can be applied to an attractive-mode operation by selecting a demand value of mechanical load-angle to be slightly smaller than half the pole-pitch.

This paper presents electromechanical dynamic simulations of a superconducting LSM rocket launcher system which is operated in an attractive-mode with control of the Coriolis force. Dynamic simulations of the ascent of the 4-ton-launcher with a 1-ton-rocket are carried out to meet the same acceleration pattern of quick acceleration and deceleration rates as that of the repulsive-mode operation used in our previous papers [1], [2]. After the rocket is released at a peak speed of about 900 km/h, the linear launcher is stopped in a very short time of 5 s by a rapid control of deceleration. During the deceleration phase, the launcher is controlled quite stably with no deflection in the center of the guide shaft while it showed an under-damped oscillation in the repulsive-mode operation. The maximum value of armature-current at a peak speed of 900 km/h is decreased to a great extent as compared with that in the repulsive-mode operation.

Electrical dynamics of induced voltages and terminal voltages are simulated when the armature-windings of the 1,500-m-long stator are all excited as one section for power supply. Electrical efficiency and power factor are also evaluated qualitatively for a more practical feasibility study. The design of section lengths greatly influences electric power, power factor and efficiency of the LSM rocket launcher system. The section length should be designed taking into account its important dependence on launcher speeds. It is shown from comparison with a one-section power supply system that an optimal design of all the section lengths along the long-stator guideway leads to high efficiency and power factor of the system.

SUPERCONDUCTING LSM ROCKET LAUNCHER SYSTEM

Figure 1 shows a concept of a large-scale superconducting LSM-controlled rocket launcher system, which has the acceleration guide tube of about 1,500 m deep under the ground. The concept is based on our theoretical works on a superconducting LSM-controlled ground-based zero-gravity facility with the drop shaft of about 800 m [3]. In Fig. 1, the LSM armature-windings installed all along the acceleration guide tube are used to drive and guide the linear launcher.

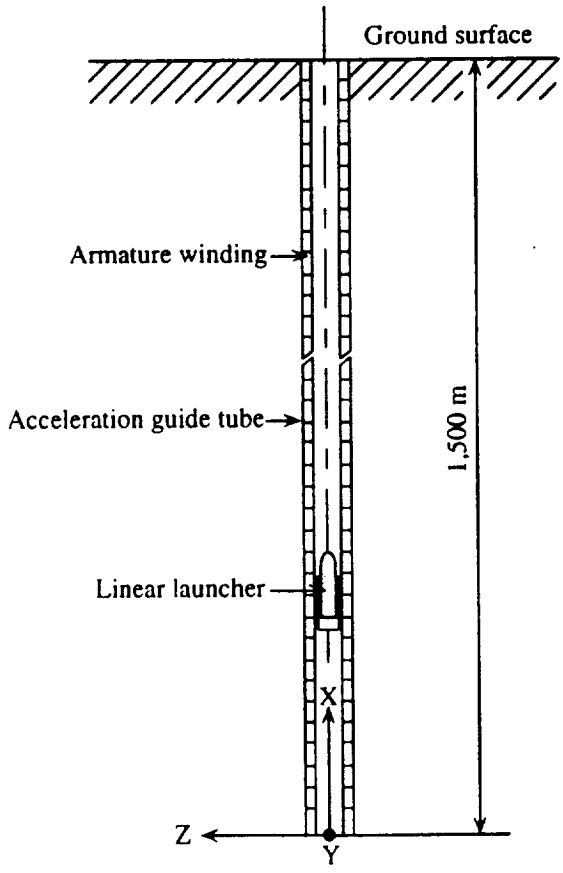

Figure 1. Vertical type superconducting-LSM controlled rocket launcher system.

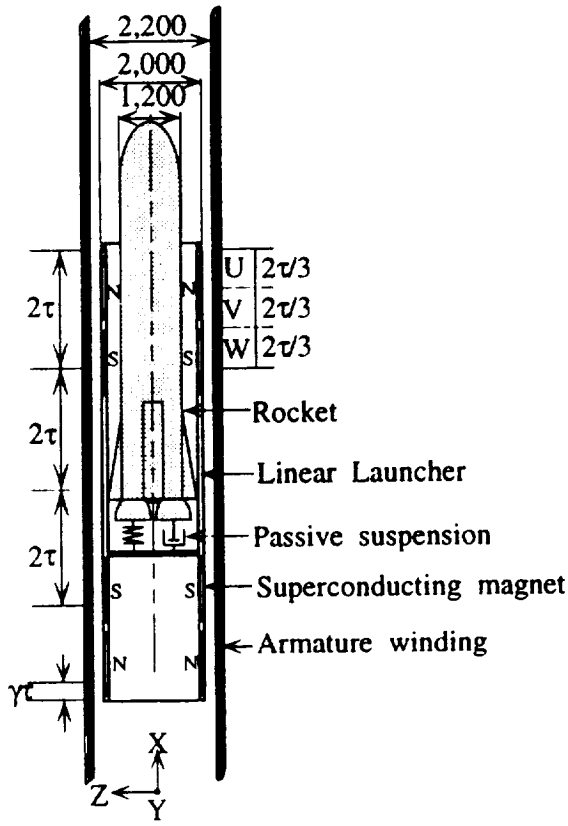

Figure 2. Acceleration guide tube of LSM armature and rocket launcher with superconducting magnets.

Figure 2 shows double-layer windings of the LSM armature which are composed of inside and outside coils, and the linear launcher on which the rocket is mounted through the use of passive suspension. The superconducting magnets are arranged with two poles facing the armature-windings in the front and rear portions of the linear launcher vehicle.

Figure 3 shows a cylindrical configuration of the LSM launcher system which has four LSM's in symmetrical positions to produce guidance forces in the Y- and Z-directions. In the figure, the linear launcher is deflected by ΔY in the Y-direction and by ΔZ in the Z-direction. Inside and outside coils of each LSM armature are connected in series and each LSM is controlled independently using each armature-current in their coils.

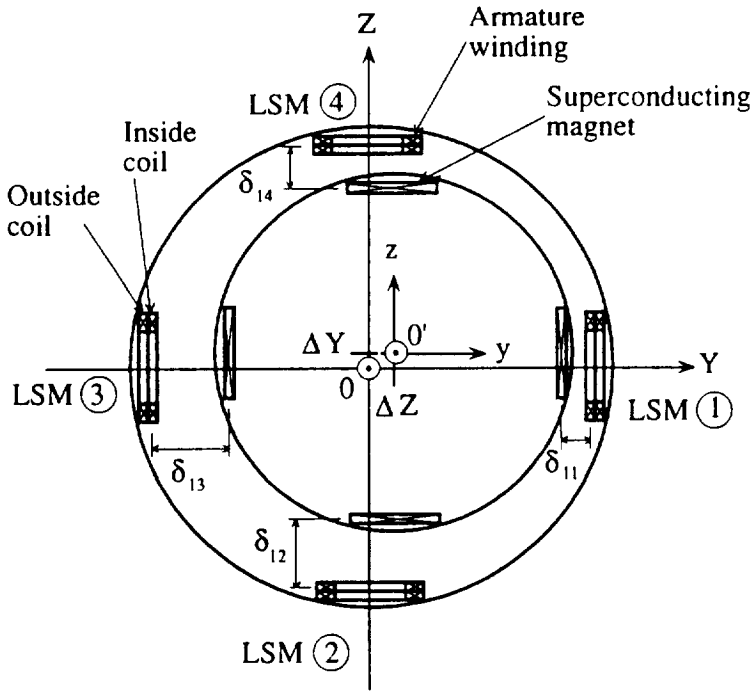

Figure 3. Model for analysis of rocket launcher showing cross-section of acceleration guide tube and four LSM's.

ASCENT AND GUIDANCE MOTION CONTROL OF LINEAR LAUNCHER AND ROCKET

The linear launcher is accelerated to a peak speed, loaded with the rocket, and after releasing the rocket, it is decelerated with no-load to be brought to rest at the end of guide tube near the earth's surface. On the other hand, during the acceleration phase, the rocket is fixed to the launcher through a passive suspension, but after separation from the launcher, it ascends freely in the guide tube. According to the armature-current control method proposed in Reference (1), the ascending motions in the X-direction of the launcher and the rocket are controlled together with the guidance motions in the Y-Z plane. When the Z-axis is assumed to be in an eastward direction, the Coriolis force can be taken into account as an external disturbance force in the Z-directed motions of the linear launcher and the rocket.

After the rocket is released from the launcher and takes off with a high initial-speed, the

rocket continues to ascend with no control subject to the Corioli's force in the Z-direction under the force of gravity in the X-direction.

The effective value of armature-current for each LSM in Fig.3 is controlled to meet the command acceleration pattern. The linear launcher should be controlled simultaneously to ascend at the synchronous speed V_{X0} of the travelling magnetic field, by producing the LSM thrust F_X. The mechanical load-angle is controlled for all the four LSM's to produce the sufficiently strong attractive force due to the resultant guidance forces F_Y and F_Z. When the launcher receives any disturbance forces in the Y- and Z-directions, the LSM guidance forces can compensate automatically and keep it at the center of the four LSM's.

ANALYSIS OF ELECTRICAL DYNAMICS

For an arrangement of the four superconducting LSM's shown in Fig. 3, each LSM can be treated independently from the viewpoint of electrical dynamics. In any LSM, a voltage equation is described for 6 armature-windings of inside and outside 3-phase-windings. Under the condition that 3-phase armature-windings and supplied voltages are all balanced and inside and outside windings are connected in series, a system of voltage equations for an arbitrary section-length is derived in the following matrix form:

$$\begin{bmatrix} v_u \\ v_v \\ v_w \end{bmatrix} = 2R \begin{bmatrix} i_u \\ i_v \\ i_w \end{bmatrix} + \frac{d}{dt} \begin{bmatrix} 2(L - M_2 + M_4) & M_5 + M_6 & M_5 + M_6 \\ M_5 + M_6 & 2(L - M_2 + M_4) & M_5 + M_6 \\ M_5 + M_6 & M_5 + M_6 & 2(L - M_2 + M_4) \end{bmatrix} \begin{bmatrix} i_u \\ i_v \\ i_w \end{bmatrix} + \begin{bmatrix} e_{u01} + e_{u02} \\ e_{v01} + e_{v02} \\ e_{w01} + e_{w02} \end{bmatrix} \quad (1)$$

where
v_v = instantaneous value of v-phase terminal-voltage
i_v = instantaneous value of v-phase armature-current
e_{v01}, e_{v02} = instantaneous value of v-phase induced-voltage in inside and outside windings
R = resistance per phase of inside or outside armature-windings
L = self inductance per phase of inside or outside armature-windings
M_2 = mutual inductance between neighbouring inside and outside armature-windings
M_4 = mutual inductance between inside and outside armature-windings of the same phase
M_5, M_6 = mutual inductance between inside and outside armature-windings of lagging and leading phases
v = u, v, w

Note that the mutual inductances M_2, M_5 and M_6 can be referred to Fig. 4.

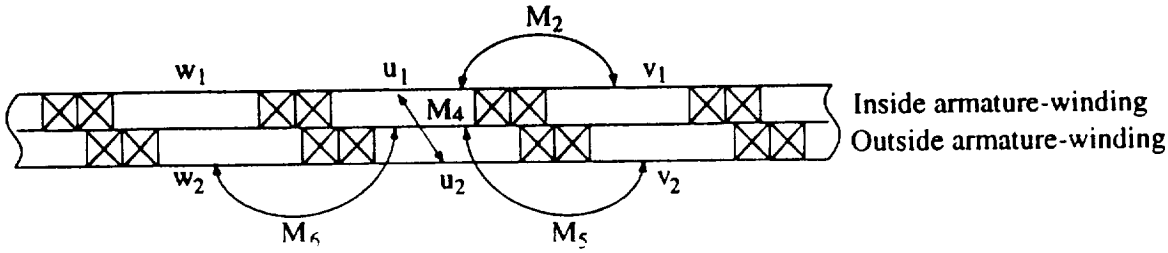

Figure 4. Mutual inductances with respect to u-phase armature-winding.

In the 3-phase armature-windings connected to satisfy the condition of $i_u + i_v + i_w = 0$, each phase-voltage equation is decoupled according to equation (1). By applying vector analysis, the terminal voltage per phase $\dot{V}$ is derived in the following vector expression:

$$\dot{V} = 2R\dot{I} + 2j\omega\left(L - M_2 + M_4 - \frac{M_5 + M_6}{2}\right)\dot{I} + \dot{E}_0 \tag{2}$$

with

$$\dot{E}_0 = E_0\, e^{j(\pi/2 - \pi/\tau\, x_0)} \tag{3}$$

where $\dot{I}$ = vector of phase current
$\dot{E}_0$ = vector of induced voltage
E_0 = effective value of induced voltage
x_0 = mechanical load-angle
$\omega = 2\pi f$ = angular velocity
f = supply frequency

The active power P_o, power loss P_l and the reactive power P_Q for each LSM system are described as follows:

$$P_o = 3E_0 I \sin\frac{\pi}{\tau}x_0 \tag{4}$$

$$P_l = 6RI^2 \tag{5}$$

$$P_Q = 6\omega\left(L - M_2 + M_4 - \frac{M_5 + M_6}{2}\right)I^2 + 3E_0 I \cos\frac{\pi}{\tau}x_0 \tag{6}$$

where I = effective value of phase current.

Apparent power P_a, the efficiency η and power factor $\cos\phi$ are thus calculated using equations (4) - (6).

$$P_a = \sqrt{(P_o + P_l)^2 + P_Q{}^2} \tag{7}$$

$$\eta = \frac{P_o}{P_o + P_l} \times 100 \tag{8}$$

$$\cos\phi = \frac{P_o + P_l}{P_a} \times 100 \tag{9}$$

DESIGN OF SECTION-LENGTH

It is of practical significance to design the section-length of the long-stator along the guideway which depends strongly on launcher speeds. Before the launcher enters the next section, the armature-current in that section is required to be at a steady state. The time constant is the same in all sections, so that the more the speed of the launcher increases, the larger the section-length should be. Figure 5 shows a design of section-length which includes 19-divisions with 30-, 60-, and 99-m-sections. The three regions of different section-length are

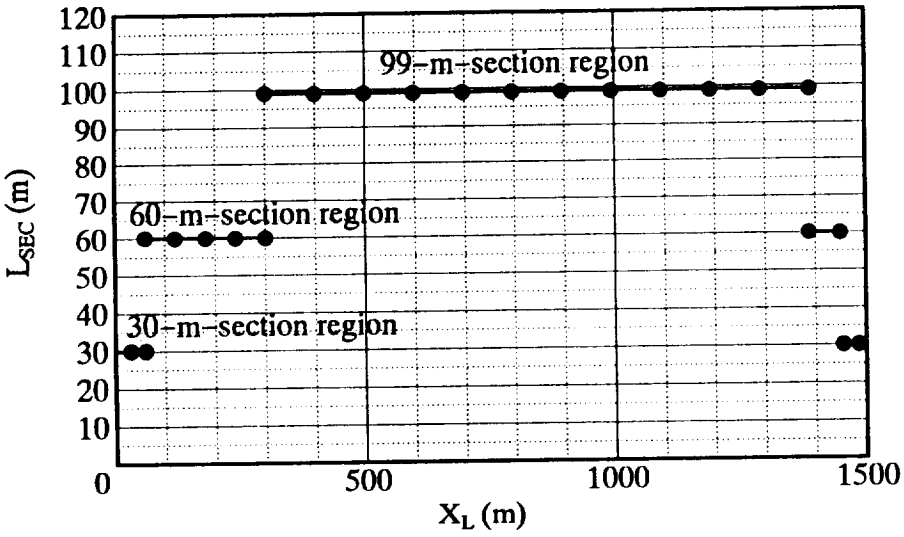

Figure 5. The 19 sections designed along the guideway

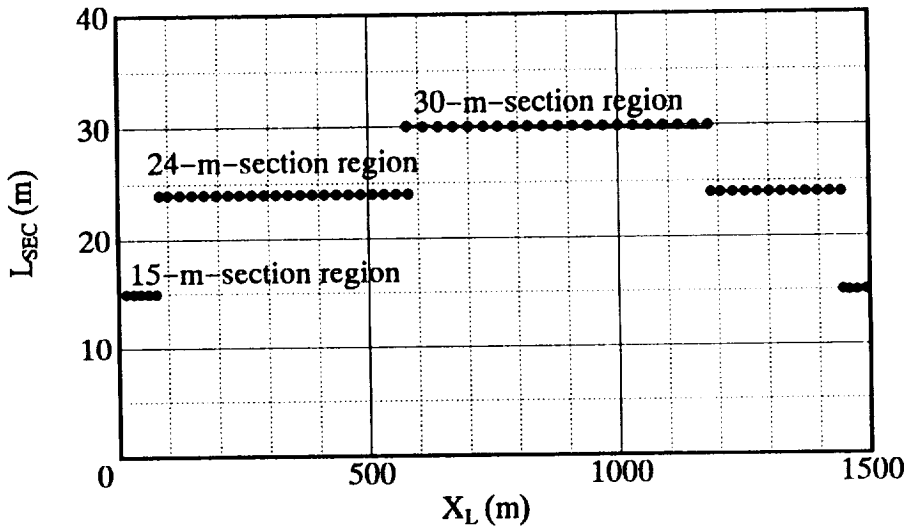

Figure 6. The 60 sections designed along the guideway

determined using the time (170 ms) enough to converge switch-on-transient phenomena, which is about five times larger than the time constant $\tau = 32.9$ ms as shown in Table 1. Figure 6 shows an optimal design of section-length which includes the 60 divisions with 15-, 24-, and 30-m-sections. This is

Table 1. Resistance, inductances and time constant in each section

section / parameter	30-m-section	60-m-section	99-m-section
R (Ω)	0.1176	0.2352	0.3881
L - M_2 + M_4 (mH)	4.8000	9.5990	15.8300
M_5 + M_6 (mH)	0.1874	0.3748	0.6185
τ (sec)	0.0329	0.0329	0.0329

calculated for the time constant of $\tau = 32.9$ ms. Even for a short time of 32.9 ms, the armature-current can be excited sufficiently by supplying a suitable voltage smaller than its maximum value which is required at a peak speed of 900 km/h.

NUMERICAL EXPERIMENTS

The superconducting LSM rocket launcher system (see Table 2) is designed for the 1-ton rocket to attain a speed of 700 km/h at the height of 100 m above the ground. In the limited length of LSM armature guide tube, the linear launcher is controlled to meet the command acceleration pattern, which has the 6.6-s-acceleration-phase with a quick variation from zero to 4 G's for 0.5 s and 4 G's kept for 6.1 s, and the 4.67-s-deceleration-phase with a very quick variation from 4 G's to -7.5 G's for 1.3 s, -7.5 G's kept for 2.87 s and a very quick variation from -7.5 G's to zero for 0.5 s.

Simulated Motions of LSM Launcher and Rocket

Fig. 7 (a) and (b) show that the rocket is released from the launcher just after the peak speed at the location of 1,000 m, launches with an initial speed of about 900 km/h, flies out the LSM guide tube with a speed of about 720 km/h and then attains the command speed of 700 km/h at the height of 100 m above the ground. An instance when the rocket is released is known from an instance for $\Delta H = 0$ in Fig. 7 (d). As shown in Fig. 7 (c), the launcher is controlled to follow very well the command acceleration pattern according to the command mechanical load-angle in Fig. 7 (e). The required armature-current and thrust force are shown in

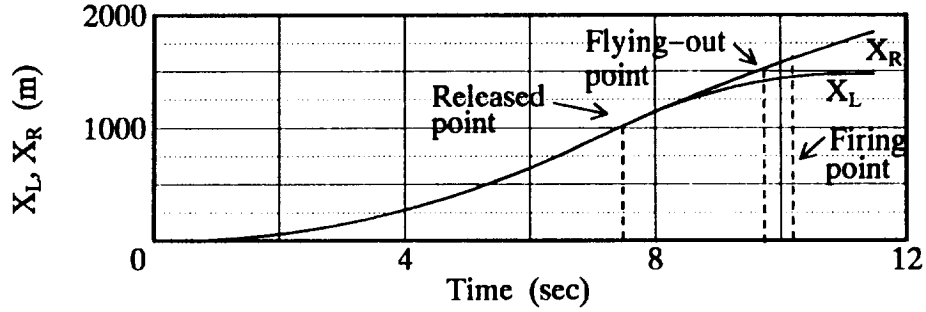

(a) Positions of ascending launcher and rocket

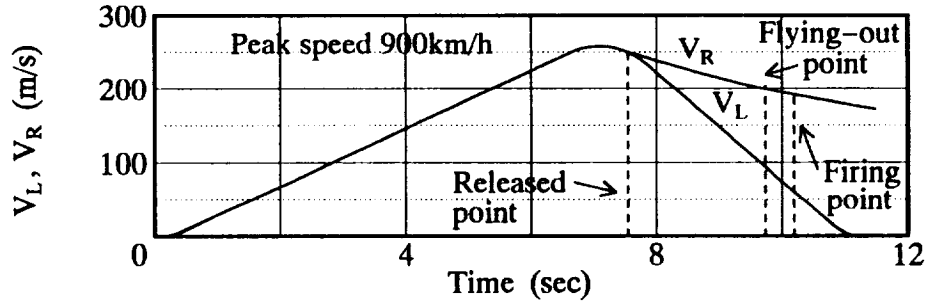

(b) Speeds of ascending launcher and rocket

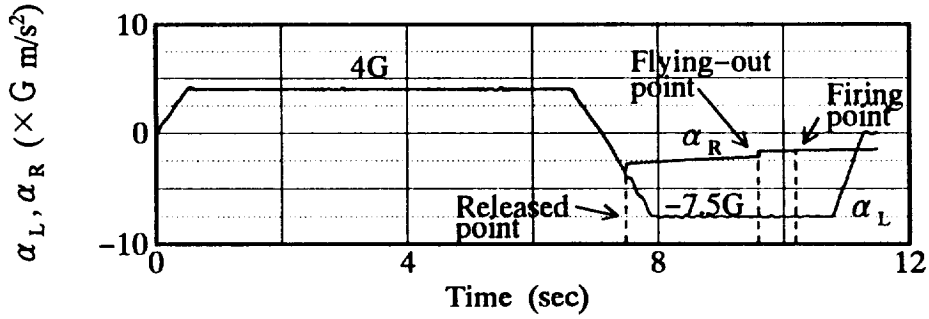

(c) Acceleration of ascending launcher and rocket

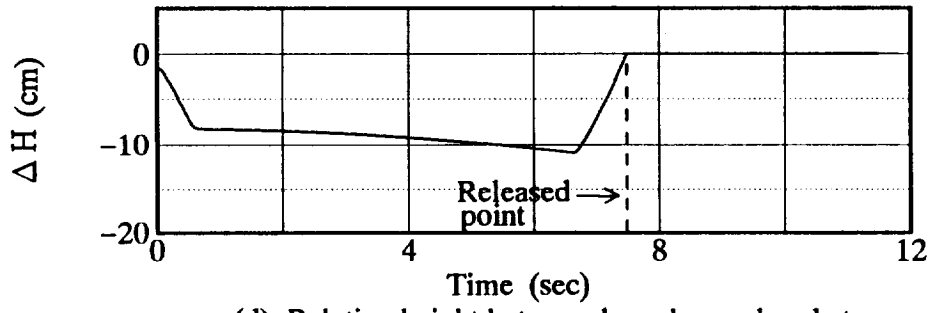

(d) Relative height between launcher and rocket

Figure 7. Ascending motion of LSM rocket launcher

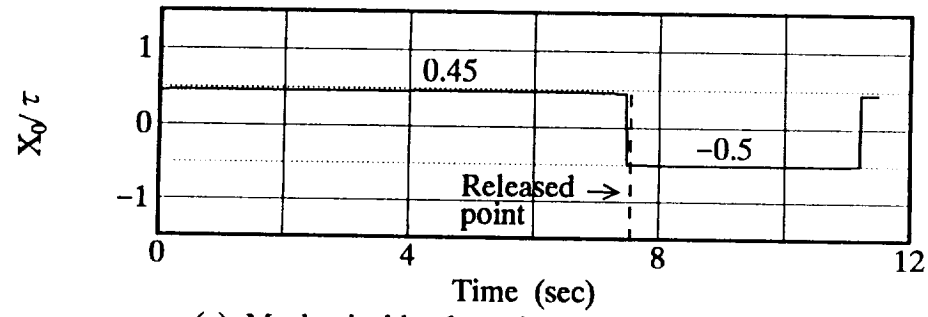

(e) Mechanical load-angle of inside armature winding

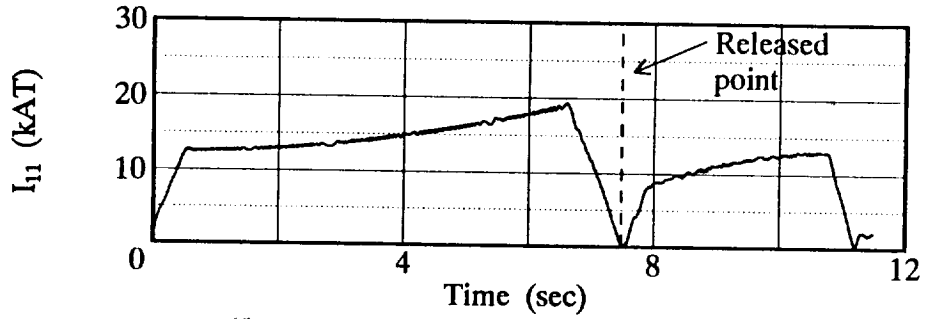

(f) Current of inside armature-winding in LSM①

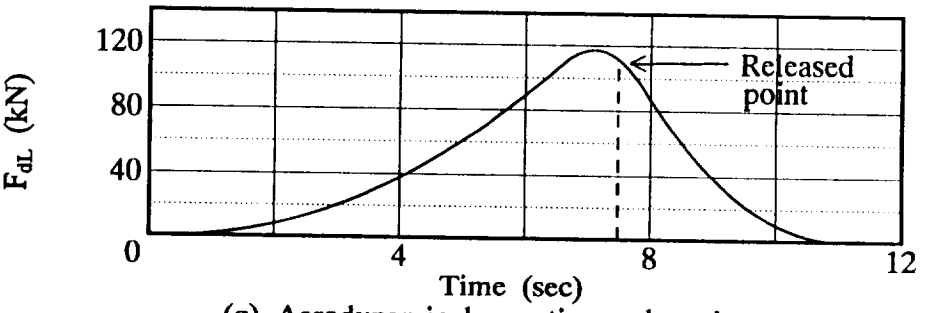

(g) Aerodynamic drag acting on launcher

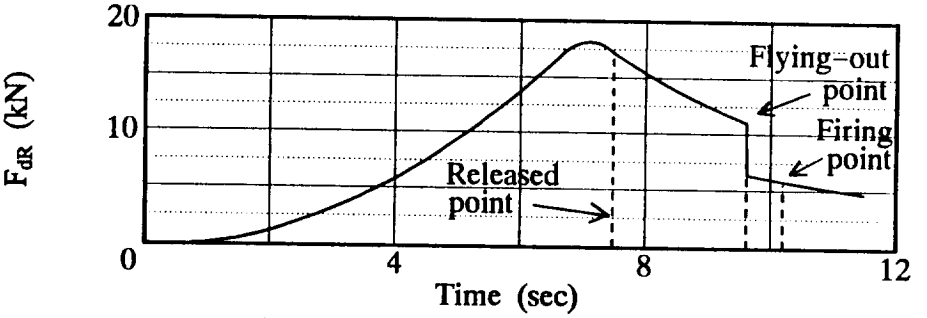

(h) Aerodynamic drag acting on rocket

Figure 7. Ascending motion of LSM rocket launcher

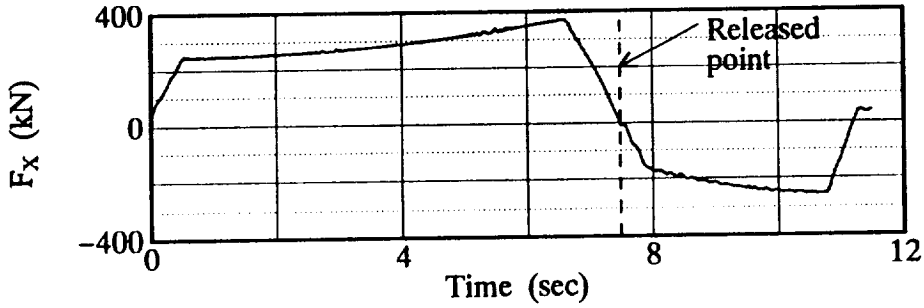

(i) Total thrust force in the X-direction

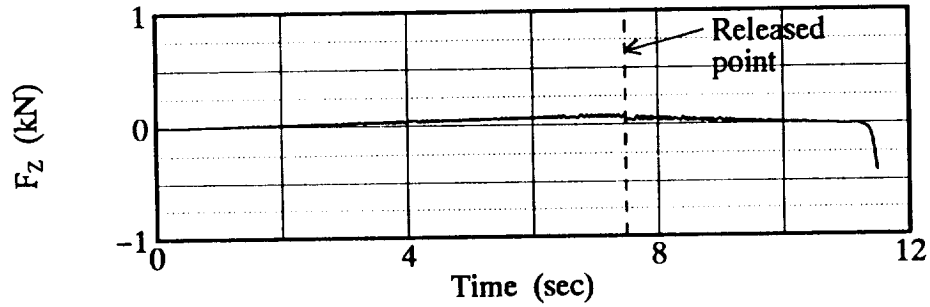

(j) Total guidance force in the Z-direction

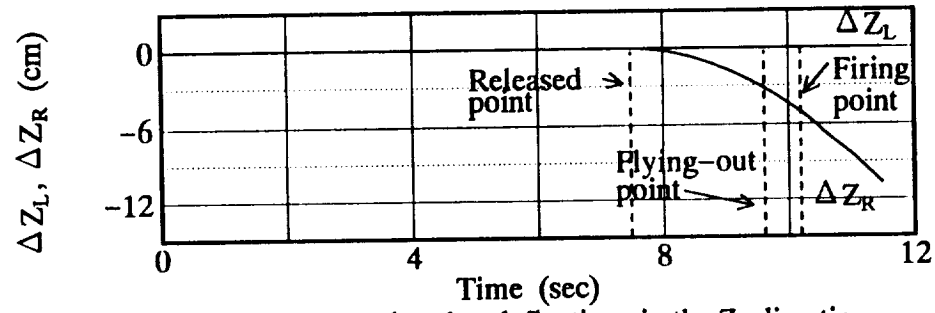

(k) Launcher and rocket deflections in the Z-direction

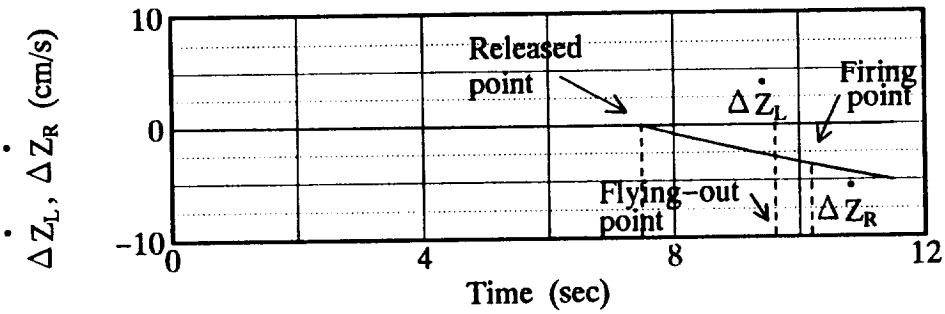

(l) Launcher and rocket speeds in the Z-direction

Figure 7. Ascending motion of LSM rocket launcher

Figs. 7 (f) and (i).

Table 2. Design data of superconducting LSM rocket launcher.

Guide Tube :		Total weight	4 ton
Total length	1,500 m	No. of Superconducting Magnets	16
Diameter	4 m	Superconducting Magnets per one LSM :	
LSM Armature Guide Tube :		No. of poles	4
Total length	1,500 m	Coil length	1.3 m
Inside diameter	2.4 m	Coil width	0.5 m
Outside diameter	2.6 m	MMF	700 kAT
No. of LSM Armature	4	Pole pitch	1.5 m
Coil length	0.8 m	Rocket :	
Coil width	0.6 m	Total weight	1 ton
Linear Launcher :		Clearance Gap :	
Total length	9 m	Electrical gap between coil centers	20 cm
Diameter	2 m	Mechanical gap	10 cm

Figure 7 (k) shows that the Coriolis force in the Z-direction is compensated completely using the guidance force in Fig. 7 (j) before the release point and after that the launcher itself is controlled quickly and stably in the center of the LSM guide tube while the rocket is deflected in the reverse direction of the Z-axis, *i. e.* in the westward direction, by 3.8 cm at the flying-out point of the guide tube end. The deflection is sufficiently small compared with the mechanical clearance between the rocket and the inside coil of LSM armature, such that the rocket does not come into collision with the wall of the inside coils. Figure 7 (l) shows that the launcher makes no motion in the Z-direction and the rocket is moved quite slowly in the westward direction due to the Coriolis force.

Electrical Dynamics Simulations

Figure 8 shows simulated results for terminal voltage, active-, reactive- and apparent-powers, power loss, efficiency and power factor per LSM in a basic case of a one-section power supply system where the 1500-m-long-stator of armature-windings are all excited simultaneously. The terminal voltage per phase becomes a maximum value of 180 kV at a peak speed of 900 km/h, as shown in Fig. 8 (a). It is known from Figs. 8 (b), (c), (d) and (e) that reactive power P_Q and apparent power P_a are about 1,000 MVA and are extremely large as compared with the active (output) power P_0 of 25 MW and power loss P_l of 47.5 MW. As a result, efficiency and power factor are generally very low, as shown in Figs. 8 (f) and (g). Figure 9 shows very important effects of section-length on electro-dynamical performance characteristics as mentioned concerning Fig. 8. It is found from Fig. 9 (a) that the maximum value of terminal voltage can be decreased by 79 % and 90 % by adapting the 19-section and 60-section power supply systems where the long-stator for each LSM is divided into 19 and 60 sections along the guideway as shown in Figs. 6 and 7, respectively. As the section-length becomes shorter, resistance and leakage inductances become smaller and reactive power P_Q and power loss P_l are dramatically decreased with active power P_0 kept constant as shown in Figs. (c), (d) and (e). Consequently, efficiency η

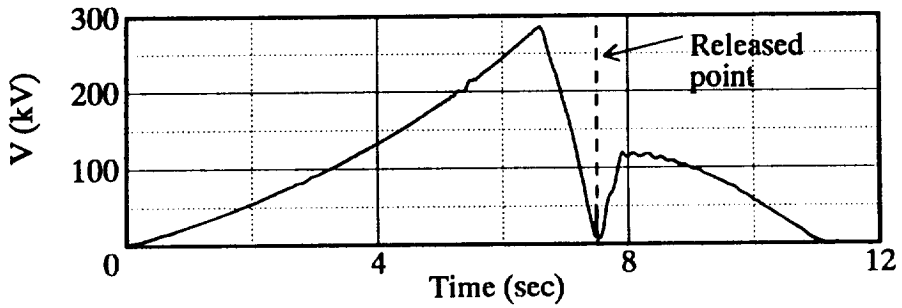

(a) Terminal voltage per phase

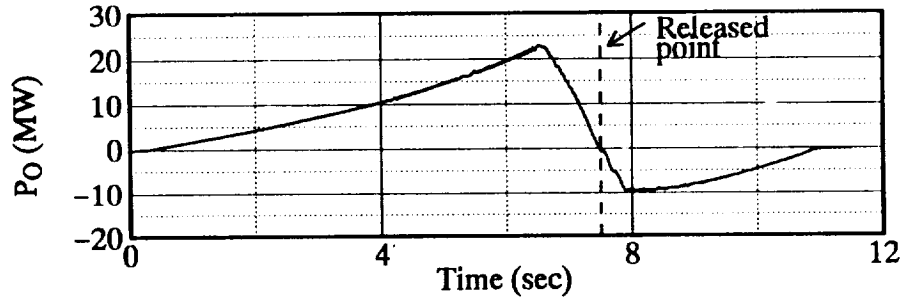

(b) Active power

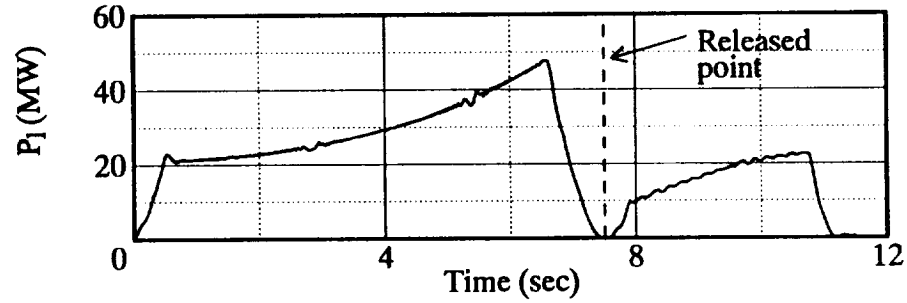

(c) Power loss

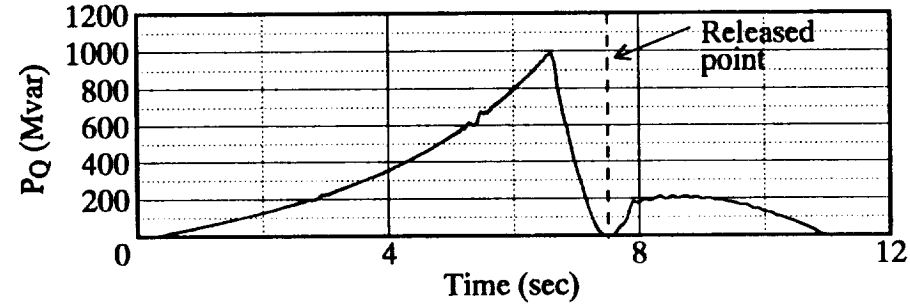

(d) Reactive power

Figure 8. Terminal voltage and electric powers in one-section power supply system

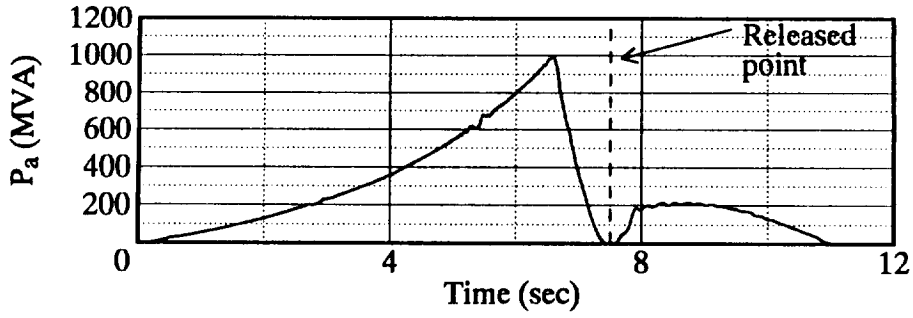

(e) Apparent power

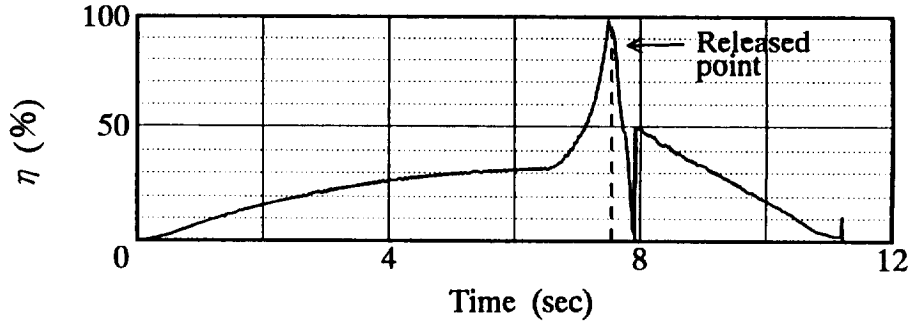

(f) Efficiency

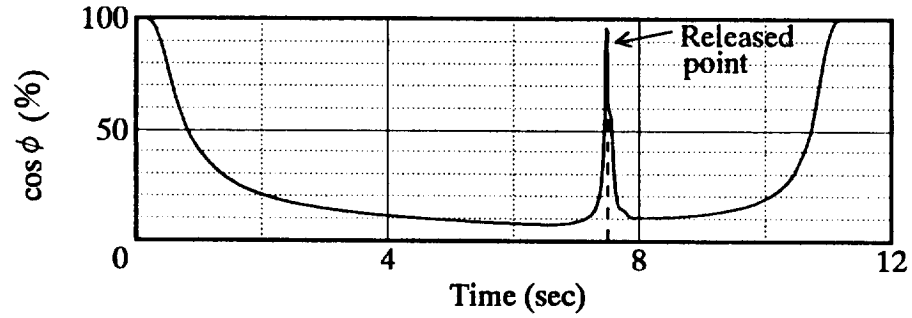

(g) Power factor

Figure 8. Terminal voltage and electric powers in one-section power supply system

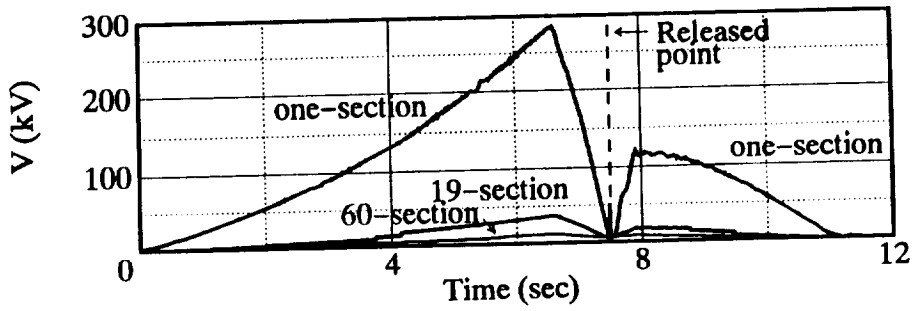

(a) Terminal voltage per phase

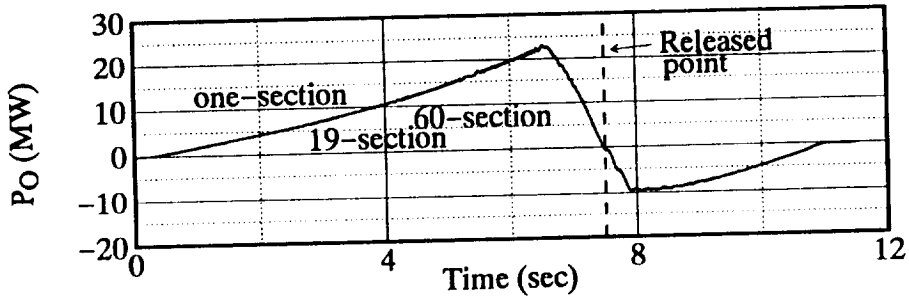

(b) Active power

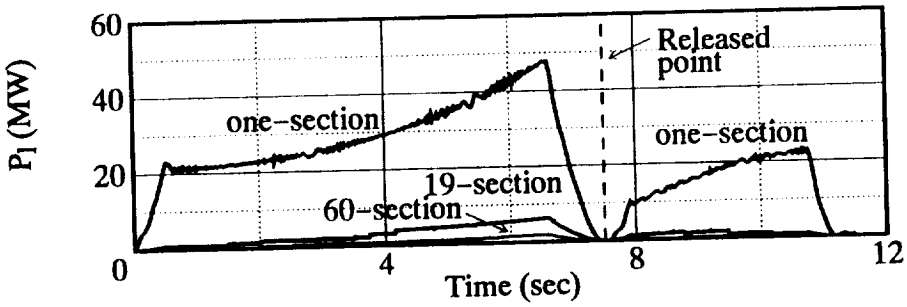

(c) Power loss

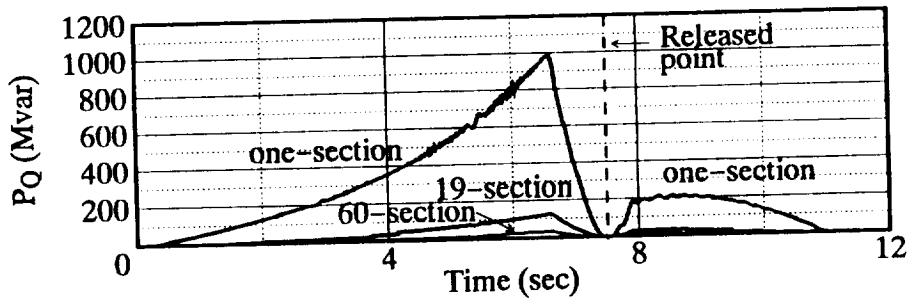

(d) Reactive power

Figure 9. Comparison of terminal voltage and electric powers among one- ,19- and 60-section power supply systems

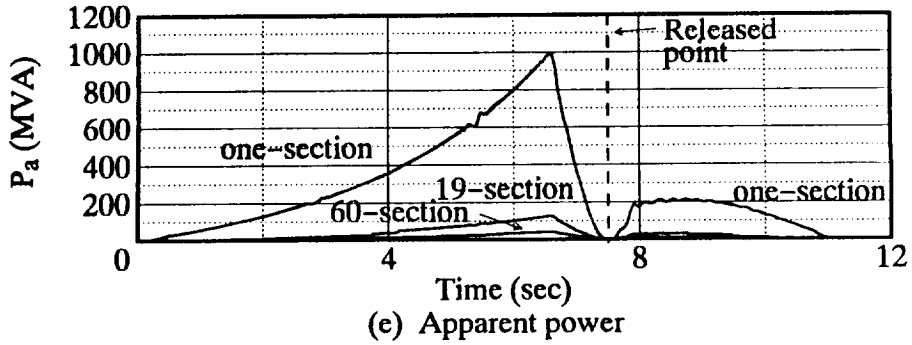

(e) Apparent power

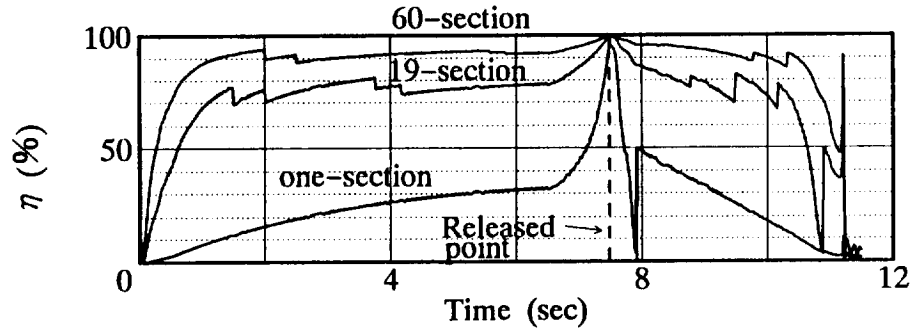

(f) Efficiency

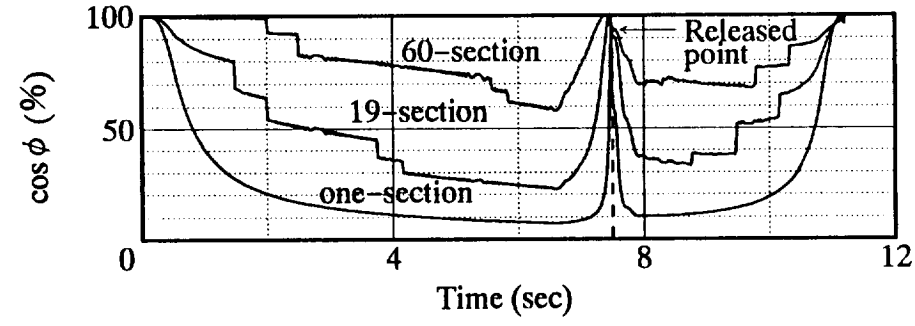

(g) Power factor

Figure 9. Comparison of terminal voltage and electric powers among one- ,19- and 60-section power supply systems

and power factor cos ϕ can be increased considerably as shown in Figs. 9 (f) and (g). Most notably, the 60-section power supply system can maximize power factor to obtain its value of 60% at lowest as compared with 22-%-power factor in the 19-section power supply system.

CONCLUSIONS

A vertical type superconducting LSM rocket launcher system under the ground which is operated in an attractive-mode is proposed and an optimal section-length of the long-stator is designed in a practical feasibility study. A computer program for simulating electromechanical dynamics of the system is developed by which the section-lengths can be designed optimally all along the guideway taking into account their dependence on the launcher speeds.

The following results are obtained from the simulation study :

(1) The novel armature-current control method proposed previously by us was also successfully applied in an attractive-mode operation for the 4-ton-launcher with 9-ton-rocket to meet the same acceleration pattern as that of the repulsive-mode used in our previous papers.

(2) The launcher is controlled quite stably with no deflection in the center of the guide shaft while compensating the Coriolis force, especially during the deceleration phase when it showed an under-damping oscillation in the repulsive-mode operation. The maximum value of armature-current at a peak speed of 900 km/h is also deduced to 73 % as compared with that in the repulsive-mode operation.

(3) The maximum values of terminal voltage per phase and apparent power for each LSM become 180 kV and 1,000 MVA and efficiency and power factor for the system are also 31 % and 8 % in a basic case of one-section power supply system. It is found that an optimal design of the 60-section-length power supply system enable the system to obtain 15 kV, 40 MVA, 92 % and 60 % for terminal voltage per phase, apparent power, efficiency and power factor, respectively.

REFERENCES

1. K. Yoshida, T. Ohashi, K. Shiraishi and H. Takami : Feasibility Study of Superconducting LSM Rocket Launcher System, NASA Conference Publication 3247 Part 2, May 1994, pp. 607 - 621
2. K. Yoshida, T. Ohashi, K. Shiraishi and H. Takami : Dynamics Simulations of Superconducting LSM Rocket Launcher System, J. of Space Tech. and Science, Vol.9 No.2, Autumn 1993, pp. 13 - 28
3. K. Yoshida, A. Kunihiro and T. Ohhashi : Superconducting LSM Dynamics in Ground - Based Zero - Gravity Facility, Proc. of Inter. Conf. on the Evolution and Modern Aspects of Synchronous Machines, Zurich, Aug. 1991, Part 3, pp. 797 - 802